The EMBO Journal vol.9 no.8 pp.2611 – 2619, 1990

Architectural organization in the interphase nucleus of the protozoan *Trypanosoma brucei*: location of telomeres and mini-chromosomes

Hui-Min M.Chung, Cathy Shea[1], Scott Fields[2], Robert N.Taub[2] and Lex H.T.Van der Ploeg[4]

Department of Genetics and Development and [2]Department of Medicine, College of Physicians and Surgeons, Columbia University, New York, NY 10032, USA

[1]Present address: Department of Brain and Cognitive Science, MIT Cambridge, MA 02139, USA

and Doris B.Tse

Laboratory of Lymphocyte Cell Biology, Department of Medicine, North Shore University Hospital and Cornell University Medical College, Manhasset, NY 11030, USA

[4]Corresponding author

Communicated by B.Pernis

We studied the spatial organization of chromatin in the interphase G1, S and G2 nucleus of the protozoan *Trypanosoma brucei*, applying *in situ* hybridization with conventional fluorescence and confocal scanning optical microscopy. The majority of the trypanosome telomere GGGTTA repeats from different chromosomes were found clustered together, either extending in a network through the nuclear interior or localized at the nuclear periphery. The population of one hundred mini-chromosomes was often asymmetrically located: either clustered in a narrow band in close association with the nuclear envelope or distributed into several clusters that segregated into roughly one half of the nucleus. The nuclear organization may undergo modifications during the cell cycle and development. We conclude that non-random spatial positioning of DNA exists in the nucleus of this protozoan. Finding a high level of structural organization in the interphase nucleus of *T.brucei* is an important first step towards understanding chromosome structure and functioning and its role in the control of gene expression.

Key words: interphase/mini-chromosome/nuclear structure/telomere/*Trypanosoma brucei*

Introduction

The overall spatial distribution of chromatin in the interphase nucleus is assumed to be random. However, it is well established that chromatin is organized into condensed and decondensed regions anchored by proteins in the nuclear matrix. Telomeres and centromeres are thought to be located at opposite poles of the nucleus (Rabl, 1885; Foe and Alberts, 1985; Comings, 1980; Hancock and Hughes, 1982; Newport and Forbes, 1987).

In a series of elegant experiments, Sedat and co-workers studied the organization of *Drosophila* salivary gland polytene chromosomes by *in vivo* DNA staining, followed by light microscopic nuclear dissection and image analysis. The polytene chromosomes exhibited right-handed coils and inter-distance maps of the chromosome arms indicated specificity in their nuclear positioning (Agard and Sedat, 1983; Mathog *et al.*, 1984; Hochstrasser and Sedat, 1987; Mathog and Sedat, 1989).

The use of biotinylated DNA probes coupled to *in situ* hybridization locates unique DNA and RNA sequences and has given some preliminary insights into the potential extent of spatial organization in the nucleus. Lawrence and co-workers showed that the spatial positioning of the locus containing the integrated Epstein Barr Virus (EBV) genome in Namalwa cell nuclei was not random (Lawrence *et al.*, 1988). Analysis of the nuclear positioning of several human chromosomes in neuronal cells indicated specificity in their location in interphase nuclei (Borden and Manuelidis, 1988). Transcripts from the EBV genome were located in organized tracks, presumably oriented for transport towards the nuclear envelope (Lawrence *et al.*, 1989). Splicing and spliceosome assembly may be compartmentalized in the nucleus as evidenced by the localization of acetylcholine receptor pre-mRNA at the nuclear membrane (Berman *et al.*, 1990). Finally, factors required for spliceosome assembly were localized to discrete regions in the nucleus (Fu and Maniatis, 1990).

The parasitic protozoan *Trypanosoma brucei* is transmitted between mammalian hosts by an insect vector, the tsetse fly. In its insect vector, the trypanosome differentiates from the bloodstream form to the insect form resulting in extensive developmental changes. Our interest is to determine the extent of topographical organization of chromatin in the interphase nucleus of the protozoan parasite *T.brucei* and to determine the potential significance of nuclear organization for nuclear functioning and the control of differential gene expression. Ultrastructural analysis of the nuclei of

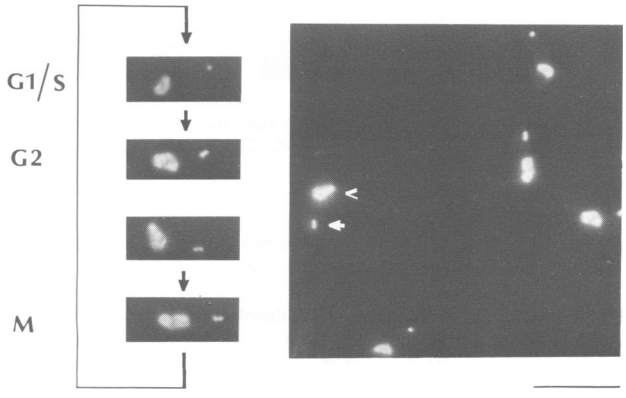

Fig. 1. *T.brucei* cell cycle. Trypanosomes were transferred to slides and stained with DAPI as described in Materials and methods. A field containing trypanosomes in the G1 or S, G2 and M phase of the cell cycle is shown on the right hand side. The left hand panel shows these trypanosomes and summarizes their position in the cell cycle. The black bar represents 8 μm.

different trypanosome species revealed that, unlike higher eukaryotes, the nuclear envelope remained intact during mitosis (Solari, 1980, 1982, 1983). The diploid *T.brucei* nucleus contains ~100 mini-chromosomes of 50–150 kb and at least 18 larger chromosomes, the largest of which measures ~5.7 Mb (Borst *et al.*, 1980, 1982; Gibson *et al.*, 1985; Van der Ploeg *et al.*, 1984a and b, 1989). The chromosome ends or telomeres of these molecules share (GGGTTA)n repeats that are also found at the ends of human chromosomes (Van der Ploeg *et al.*, 1984c; Blackburn and Challoner, 1984; Cooke *et al.*, 1986; De Lange *et al.*, 1990). Many of the telomeres encode variant cell surface glycoprotein (VSG) genes and telomeric VSG genes can enter one of several telomeric VSG gene expression sites by different types of DNA recombinational events (for review see Van der Ploeg, 1990). At interphase the 120 chromosomes are located in a small, spherically shaped nucleus with a diameter of ~2.5 μm. A few kb of DNA, if fully stretched out, spans several μm, so random distribution of the 70 000 kb of DNA in the diploid *T.brucei* nucleus should lead to a heterogeneous distribution of any moderately repetitive sequence. Our present studies were aimed at determining the distribution

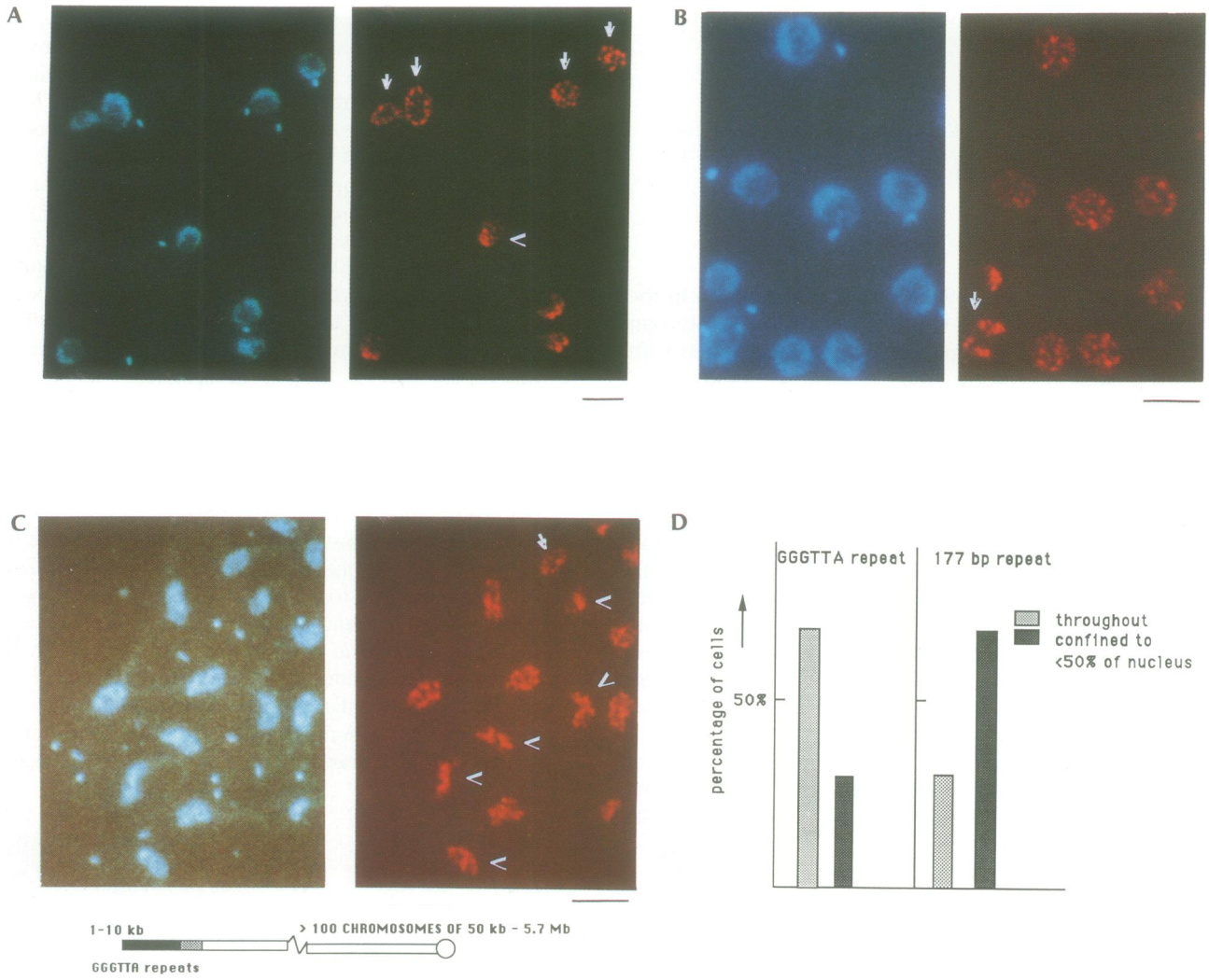

Fig. 2. *In situ* hybridization of trypanosomes with a telomere GGGTTA repetitive probe. *In situ* hybridizations of insect form trypanosomes (**panels A** and **B**) and bloodstream form trypanosomes (**panel C**) with a telomere GGGTTA repeat probe. The left hand side of each panel shows the DNA-specific DAPI stain and the right hand panel shows the rhodamine detected hybridization signals. The black bar below each panel represents 2 μm. **Panel D** presents a comparison of the distribution patterns in percentages, comparing the telomere repeat (GGGTTA)n and mini-chromosome 177 bp repeat probes for insect form trypanosome G1 and S phase nuclei. 300 nuclei were counted from four different experiments for the telomere hybridization and three different experiments for the 177 bp repeat hybridizations. The hybridization patterns were grouped into nuclei containing hybridization signals distributed throughout the entire nucleus (labeled 'throughout'), or nuclei with hybridization signals that were confined to <50% of the nuclear volume (labeled 'confined to <50% of the nucleus'). The percentages and standard errors of the telomere hybridization patterns were 79.5% ± 4.9%, for the 'throughout' pattern and 20.5% ± 4.9% for the distribution pattern confined to <50% of the nucleus. For the 177 bp repeat hybridization, the percentages of the distribution patterns were 27.9% ± 1.1% for the 'throughout' and 72.1% ± 1.1% for the distribution pattern confined to <50% of the nucleus. The *P* value for the difference between the telomere and the 177 bp repeat distribution patterns was $<<0.001$. Nuclei in either the G2 or M phase of the cell cycle were omitted from the comparison. The physical map at the bottom shows a schematic outline of the location of telomere repeats (black box), subtelomere repeats (shaded box) and the size and number of trypanosome chromosomes.

patterns of telomeres and mini-chromosomes (Sloof *et al.*, 1983; Van der Ploeg *et al.*, 1984a and c). Establishing architectural organization for the protozoan nucleus and defining nuclear structure will have implications for telomere and chromosome function, the molecular mechanisms that determine structure and control differential gene expression and DNA recombination events.

Results

Telomeres in the T.brucei interphase nucleus

In addition to its nuclear genome, *T.brucei* has a complex and unusual kinetoplast or mitochondrial genome consisting of a concatenated network of thousands of 1 kb mini-circles and tens of 20 kb maxi-circles (Englund *et al.*, 1982; Clayton, 1988). Cytofluorimetric analysis of trypanosome DNA has previously revealed that the S phase of the cell cycle was followed by a G2 phase in which the trypanosome's single mitochondrion divides (Borst *et al.*, 1980, 1982). In Figure 1, right panel, a G2 trypanosome is marked with an arrow (showing the kinetoplast) and arrowhead (nucleus). In the M phase, nuclear division occurs (Figure 1, left panel, trypanosome marked M). This finding allows the classification of almost any trypanosome that has been stained with the DNA specific dye, 4′ 6-diamidino-2-phenylindol (DAPI) into the G1 and S or the G2 or M phase of the cell cycle based on the number of kinetoplasts and nuclei per cell (Figure 1, examples are aligned in the left panel). The location of the kinetoplast relative to other cellular organelles in bloodstream form trypanosomes (Figure 1) differs from that in insect form trypanosomes (compare Figure 2B and 2C).

We hybridized nuclei of trypanosomes with biotinylated DNA probes and used tetramethyl-rhodamine-isothiocyanate (TRITC) conjugated streptavidin for probe detection. The *in situ* hybridization and fixation procedures were modified from the method of Lawrence *et al.* (1988, 1989) to give optimal results for trypanosome nuclei. The limit of detection was ~30 kb; these signals were orders of magnitude lower than the hybridization signals obtained with the repeated DNA probes (see Materials and methods for details). All results were obtained using either formalin−methanol−acetic acid or a cross-linking agent, paraformaldehyde as a fixative to preserve nuclear structure. Both techniques gave identical results indicating that structural modifications of the nuclei are not likely to have affected our observations.

The genome of *T.brucei* contains about 240 telomeres with between 1 and 10 kb of the telomere GGGTTA repeat at each telomere (Van der Ploeg *et al.*, 1984a, b and c). We hybridized insect form trypanosome nuclei with a biotinylated telomere repeat (GGGTTA)n probe and thus determined the location of at most 2.4 Mb of telomeric DNA. The distribution of telomeric DNA is indicated by a punctate staining pattern, i.e. the hybridization signals are seen as numerous, distinct, small clusters. In the majority of nuclei (>70%) the telomeric sequences were found in several clusters spread throughout the entire nucleus (Figure 2A; nuclei marked with an arrow at the extreme right side, TRITC panel, and the majority of nuclei in Figure 2B), or associated in several (>10) clusters that were uniquely located at the extreme periphery of the nucleus, indicating association with the nuclear envelope (Figure 2A, nuclei marked with arrows on the left of the TRITC panel). This peripheral distribution of the telomere repeats sometimes covered only ~300° of the nuclear circumference (see also Figure 4A, images 2 and 3). A less frequent pattern of distribution (<30%) is exemplified by the nucleus (marked with an arrowhead) in the middle of the TRITC panel of Figure 2A, in which most telomeric DNA is aggregated at one pole (see Figure 2D for quantification).

Simultaneous DAPI staining of the nuclei (left panels, Figure 2A−C) demonstrated that the nuclei were intact and in interphase (G1 and S or G2). DAPI staining also showed that the DNA is not homogeneously distributed throughout the nucleus. This DAPI staining pattern was also seen with cells stained *in vivo* and therefore represents the native distribution of genomic DNA (data not shown). However,

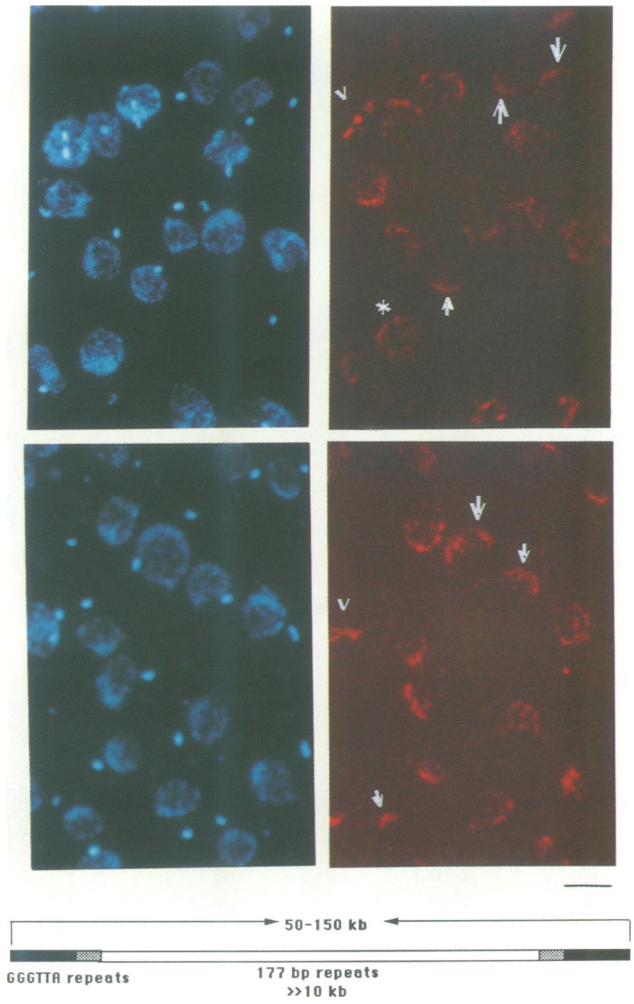

Fig. 3. Nuclear distribution of the 177 bp mini-chromosome specific repeat. *In situ* hybridizations were performed with the 177 bp mini-chromosome specific probe with insect form trypanosomes. The left panels show the DNA-specific DAPI stain, the right hand panels the rhodamine detected hybridization signal of the 177 bp repeat probe. The black bar represents 2 μm. A schematic outline of a trypanosome mini-chromosome (50−150 kb in size) is shown at the bottom. Several nuclei in which 177 bp repeat hybridization occurred to <50% of the nuclear volume are indicated with arrows. Two nuclei marked with arrowheads are in the M phase of the cell cycle. One nucleus showing a nuclear distribution of 177 bp repeats equivalent to that of the telomere repeats, i.e. throughout the entire nucleus is marked with an asterisk.

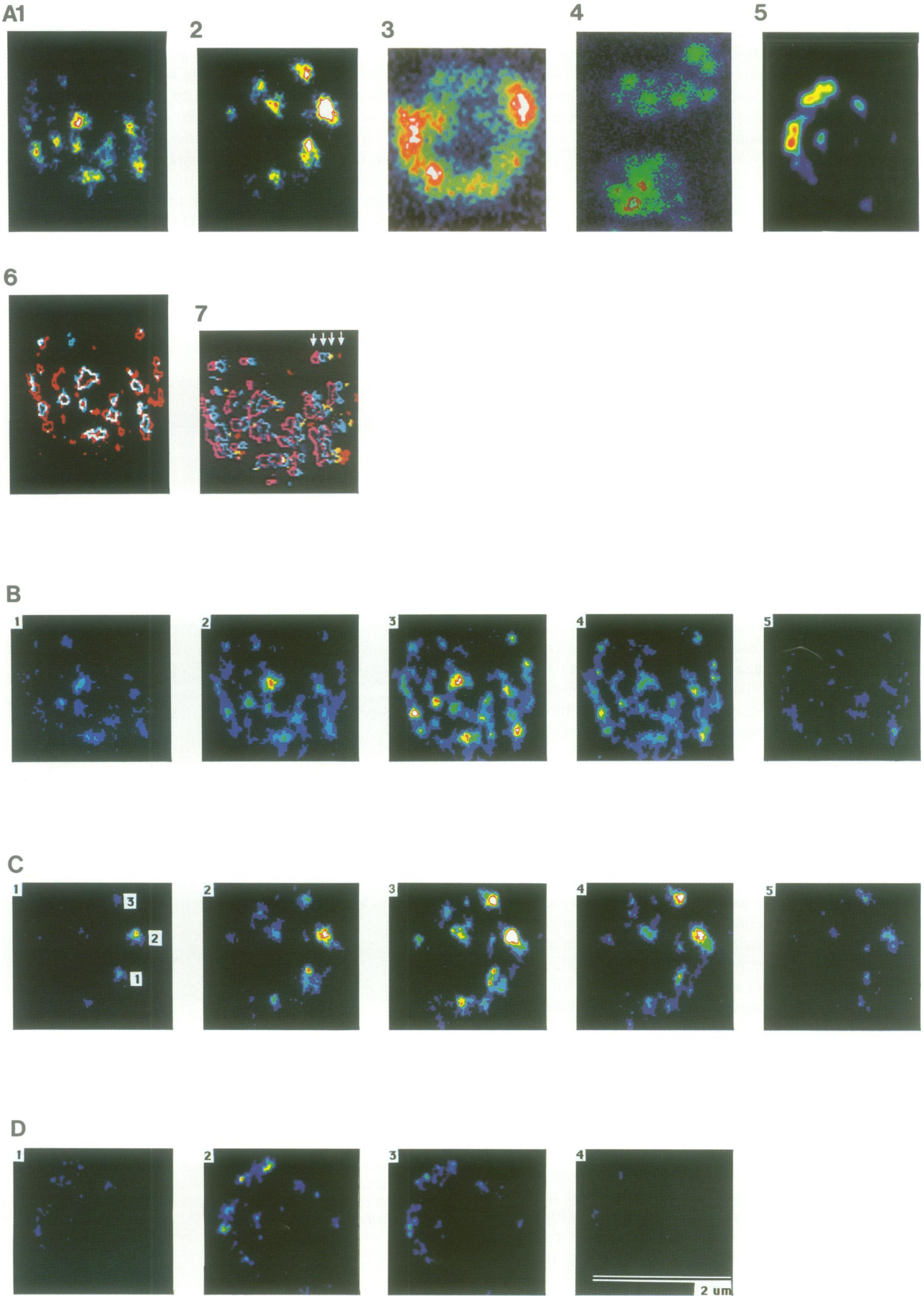
A1
2
3
4
5
6
7
B
1
2
3
4
5
C
1
3
2
1
2
3
4
5
D
1
2
3
4
2 um

the clusters of telomere repeats did not superimpose the areas of the most intense DAPI staining, indicating that telomeres were specifically compartmentalized compared to the bulk of the DNA (Figure 2A and B). For some cells superimposition of the nucleus and the kinetoplast did not allow the determination of their position in the cell cycle.

The patterns of telomere distribution showed differences when insect form (stock 427-60, Brun and Schonenberger, 1979 and stock 427-60 variant 118 clone 1, Rudenko and Van der Ploeg, 1989) and bloodstream form trypanosome nuclei (variant 118 clone 1, Lee and Van der Ploeg, 1987) were compared. Firstly, bloodstream form nuclei are smaller and are not spherically shaped (Figure 2C). Secondly, while the telomeric DNA in blood stream form cells also appeared aggregated, it showed fewer individually identifiable telomere clusters (Figure 2C, nuclei marked with arrowheads). In a small percentage of the nuclei, telomeres were distributed at the extreme periphery (Figure 2C, nucleus marked with arrow).

Mini-chromosomes in insect and bloodstream form trypanosomes

The *T.brucei* genome contains a large number (100) of unusually small, 50−150 kb, mini-chromosomes which account for ~10% of the genome. These small, mitotically stable chromosomes contain an abundant 177 bp mini-chromosome-specific repeat, extending over tens of kilobase pairs (Sloof *et al.*, 1983; Van der Ploeg *et al.*, 1984a). The 177 bp repeats represent at least 1 Mb of DNA (M.Weiden and L.H.T.Van der Ploeg, unpublished). We compared the nuclear organization of the trypanosome telomere repeat sequences with the trypanosome mini-chromosomes as visualized by the location of the 177 bp repeats. The hybridizations were performed under identical conditions to those described for the telomere repeat probe. In contrast to the telomere repeats, in the majority (>70%) of the nuclei the 177 bp repeat was clustered in less than half of the surface area of the nucleus. 177 bp repeats were either entirely clustered in a narrow band at one pole of the interphase nucleus or spread evenly in many small clusters restricted to roughly one half of the nucleus (Figure 3, nuclei marked with arrows). In a less frequent pattern of distribution, the hybridizing sequences were scattered throughout the entire surface area of the interphase nucleus in several small clusters (nucleus marked with an asterisk in the top panel). Some nuclei in the G2 phase of the cell cycle (marked with arrowheads) showed the 177 bp repeats aligned in the center, while the majority of the DNA was heterogeneously distributed throughout the nucleus (compare top left and top right panels). Our preliminary data indicate that in bloodstream form trypanosomes, the 177 bp repeats were not confined to one pole but instead were distributed throughout the nuclei (data not shown). Given the frequencies of the telomere and mini-chromosome distribution patterns (see Figure 2D for quantification and statistical significance), we conclude that the 177 bp repeats in insect form trypanosomes are distributed differently from the telomere repeats and are mostly asymmetrically located in less than one half of the nucleus.

Three-dimensional nuclear reconstruction and semi-quantification of telomere and mini-chromosomal hybridization signals

The distinct distribution patterns of the telomere and mini-chromosome repeat families revealed structural organization in the trypanosome nucleus. However, it is not possible to deduce the three-dimensional distribution of these sequences from the two-dimensional light microscopic images. Confocal scanning optical microscopy allows the optical dissection of nuclei generating individual images from different planes of a single nucleus (for review see Shotton, 1989). These images can be superimposed and the location of the hybridizing sequences in the nuclear interior reconstructed. Confocal laser microscopy and image analysis also allow quantitation of the signals from within a single nucleus. In addition, the image can be enhanced and enlarged with an accuracy that cannot be obtained with conventional microscopy and photographic techniques. We scanned through the trypanosome nuclei in steps of 0.2 μm, with a depth of field of detection of <0.2 μm (see Materials and methods for details). A self-contained computer work-station was used for data storage and image analysis. In the two-dimensional images, different colors reflect relative signal intensities ranging from black (the background) to the brightest signal, shown in white (see legend to Figure 4 for details). Ten insect form nuclei were scanned and analyzed. Data from two nuclei, hybridized with a telomere repeat probe (Figure 4A, images 1 and 2) and one nucleus

Fig. 4. Confocal optical scanning microscopy of trypanosome nuclei. Confocal optical scanning microscopy and image analysis of rhodamine hybridization signals in insect form nuclei, hybridized with a telomere repeat probe or a mini-chromosome specific 177 bp repeat probe were performed as described in Materials and methods. Differences in color in the images reflect relative signal intensities, ranging from black (the background) to dark blue, green, magenta, cyan, yellow, red and white, which represents the brightest signal (relative intensities are on a linear scale with roughly equal intervals for the intensity increase with each color). The black bar at the bottom right represents 2 μm. **Panel A** presents the hybridization of insect form nuclei with a telomere repeat probe (images 1−3, one nucleus in each image), the hybridization of two bloodstream form nuclei with a telomere repeat probe (image 4, one nucleus with five telomere clusters at the top and one nucleus with a single telomere cluster at the bottom) and one insect form nucleus hybridized with the mini-chromosome specific 177 bp repeat (image 5). Images 1−5 were generated using a wide depth of field (>5 μm). The images have been enhanced to different extents to facilitate pattern interpretation. Images 1, 2 and 5 show the brightest hybridizing regions only, while images 3 and 4 show all of the hybridization signal. The confocal optical scanning patterns of the insect form nuclei hybridized with a telomere repeat probe, shown in panel A (images 1 and 2) are presented in **panels B** and **C**, respectively. Confocal optical scanning of a nucleus hybridized with a mini-chromosome 177 bp repeat probe (panel A, image 5) is presented in **panel D**. Confocal optical scanning was performed in 0.2 μm per step with a depth of field of <0.2 μm. Only 5 scanning images, spaced 0.4 μm apart are presented, panels B and C, and 4 images, spaced 0.4 μm apart in panel D. The sequentially obtained images are numbered to facilitate their comparison. Three regions of hybridization in the images of panel C have been numbered 1−3 in image 1 to facilitate their comparison. Images 6 and 7 of panel A represent schematic models of the scanning images of the insect form nucleus shown in panel B. A superimposition of a schematic stick figure model of the hybridization patterns of image 2 and image 4 of panel B is represented in image 6 of panel A. The white areas in image 6 of panel A represent regions in which the hybridization signals of the two fields are located in identical regions and the blue and red regions reveal hybridization signals unique to images 2 and 4 of panel B, respectively. The three-dimensional reconstruction presented in panel A (image 7) shows superimpositions of the signals of images 2a (purple), 3a (blue), 4a (yellow) and 5a (red) of panel B (see text for a discussion of image 'a'). The three dimensional image was constructed by shifting the individual fields to the right, at five pixels for each superimposition. The arrows highlight a telomere repeat hybridizing region.

hybridized with the mini-chromosome specific 177 bp repeat probe (Figure 4A, image 5) are presented. The images in Figure 4A were taken with a depth of field of >5 μm. The images in Figure 4A have been enhanced and simplified to different extents to facilitate pattern interpretation. In Figure 4A, images 1, 2 and 5 show the brighter hybridizing regions, while images 3 and 4 show all of the hybridization signal. Comparison of the insect form nuclei (Figure 4A images 1, 2 and 3) and the smaller bloodstream form nuclei (Figure 4A, image 4 which contains two nuclei) shows that in bloodstream form trypanosomes, the telomere hybridizing sequences are more highly clustered and centrally located.

Narrowing the depth of field allowed scanning through the nucleus. Figure 4B and 4C show the scanning images of the nuclei in images 1 and 2 of Figure 4A, respectively. About 12 steps of 0.2 μm were needed to scan through the telomere hybridizing regions. Only 5 scanning images, spaced at 0.4 μm intervals are presented in panels B and C. The first and last images in panels B and C have been omitted to facilitate presentation. These peripheral images lacked distinct hybridization signals. Since the trypanosome nucleus has a diameter of ~ 2.5 μm and the hybridization signals spanned ~ 2 to 2.4 μm, the telomere repeats appear to extend throughout most of the nucleus. Extensive distortion of nuclear shape has not occurred but the nucleus appears flattened.

The telomere hybridization in Figure 4B started with a low level signal intensity at the ends of the nucleus and increased towards the more centrally located regions. We constructed several models of the hybridization patterns to facilitate their interpretation (examples are shown in Figure 4A, images 6 and 7). A superimposition of a schematic stick figure model of the hybridization patterns of images 2 and 4 of Figure 4B is represented in image 6 of Figure 4A. The white areas show hybridization signals of the two fields, separated by ~ 0.8 μm in the nucleus, that are located in identical regions while the blue and red areas show hybridization signals unique to images 2 and 4 of Figure 4B, respectively. This reconstruction shows that the telomere repeats extend through the interior of the nucleus with some of them in close proximity to the nuclear envelope. Specific connections exist between the brightly hybridizing areas as indicated by the light blue lines in the images in Figure 4B. These connections together with the more brightly hybridizing regions appear to generate a complicated lattice of telomere repeat sequences. In the three-dimensional reconstruction (Figure 4A, image 7) different images from Figure 4B were superimposed and shifted five pixels to the right to generate a three-dimensional projection. Colors were used to facilitate comparison of the signals from each two-dimensional field presenting the signals from image 2a in purple (the 'a' images are located 0.2 μm on top of each numbered image presented in Figure 4B), image 3a in blue, image 4a in yellow and image 5a in red. These fields spanned a region totalling 1.2 μm. The reconstruction shows telomere repeats extending in stem-like structures (one is highlighted with arrows in Figure 4A image 7) and that the distribution of telomere repeats is significantly different in almost every field.

The second most common telomere distribution pattern showed the location of telomere sequences at the periphery of the nucleus (Figure 2A; Figure 4A, images 2 and 3). Scanning one of these nuclei (Figure 4A, image 2) revealed that the telomeric sequences extend along the nuclear periphery, throughout almost the entire nucleus (Figure 4C). To facilitate comparison, three hybridizing regions have been numbered (1–3) in image 1. Hybridization signals extended through the nucleus but alternations in the distribution patterns are observed in almost each field (compare region 1 in images 2, 3 and 4). The Z axis resolution of the confocal microscope is partially dependent on the intensity of the hybridizing signals. The exact dimension of each hybridizing region is therefore difficult to determine. However, the pattern of hybridizing sequences is altered when different scanning fields are compared and we can therefore infer from our data that the telomere repeats extend along the nuclear periphery (Figure 4C), or form a network that extends through the nuclear interior (Figure 4B).

Figure 4D presents the images of a representative trypanosome nucleus hybridized with the mini-chromosome specific 177 bp repeat probe. The asymmetric 177 bp repeat distribution at one pole of the nucleus is obvious from the wide depth of field image in Figure 4A (image 5). The

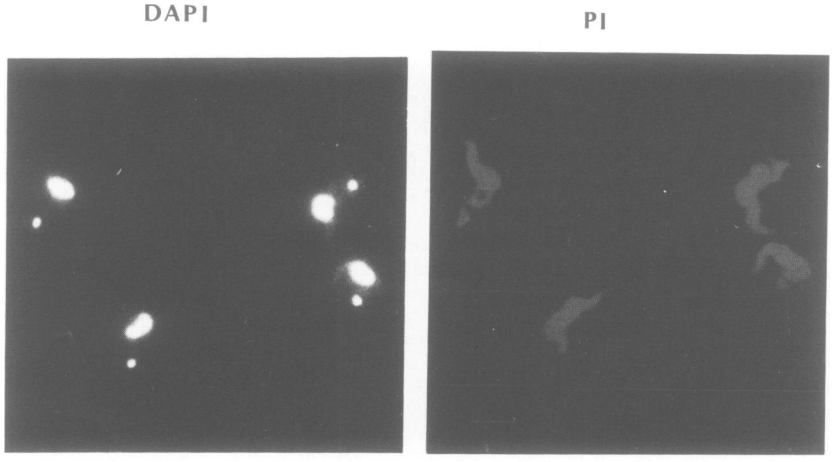

Fig. 5. Non-random positioning of trypanosomes following a cytospin. The left hand panel shows bloodstream form trypanosomes stained with the DNA-specific dye DAPI and the right hand panel shows the same trypanosomes stained with the DNA and RNA reactive dye, propidium iodide (panel PI). The black bar represents 8 μm.

confocal scanning patterns revealed that the hybridizing sequences extended along one side of the nucleus. Only faint hybridization signals could be detected in the peripheral images, 1 and 4, of Figure 4D. Mini-chromosomal 177 bp repeat sequences thus appear to form a network of DNA compartmentalized into a relatively narrow band at one pole, apparently in tight association with the nuclear envelope.

Examination of the telomere repeat hybridization patterns shows that they cannot be explained by assuming that we observe a similarly organized nucleus from different rotational angles (Figure 4 and data not shown). In addition, for the 177 bp repeat we visualized mainly nuclei with an asymmetrical distribution of the 177 bp hybridization signal, localized on one side of the nucleus (Figures 3 and 4). This pattern of 177 bp repeat hybridization cannot be explained if the nuclei are randomly positioned relative to the path of the light. These patterns indicate that we do not observe the nuclei in different trypanosomes from all possible rotational angles since it is obvious that random positioning of cells and nuclei would lead to the largest variety of images. In fact, due to the asymmetrical shape of the trypanosome, the cells are not oriented randomly and are positioned with their 8 μm long side perpendicular to the path of the light (as shown in Figure 5). The bias observed in the distribution patterns might thus be explained if the nucleus has a fixed orientation relative to the other cellular organelles. A similar conclusion has previously been drawn for the orientation of nuclei with respect to the cytoplasm in the multinucleated *Drosophila* embryos (Foe and Alberts, 1985).

Discussion

We show that the majority of telomere (GGGTTA)n repeats and the mini-chromosome 177 bp repeats, which together account for 10% of the *T.brucei* genome, are positioned in well defined regions within the interphase (G1, S and G2) nucleus of the protozoan *T.brucei*. In higher eukaryotes, telomeres have previously been shown to be associated at one pole of the nucleus with the nuclear envelope (Rabl, 1885; Foe and Alberts, 1985). In trypanosomes, this distribution pattern was observed infrequently. The telomere repeats from the 120 chromosomes were most often aggregated in several discrete regions in association with the nuclear envelope or extended through the nuclear interior. Telomere repeats are known to confer stability onto artificial chromosomes maintained in yeast (Szostak and Blackburn, 1982). The assembly of telomeres which we observed in trypanosomes could be of significance for the functioning of the telomeres, serving as anchoring sites for the chromosome ends, conferring stability onto the linear chromosomes. The molecular basis for the association of telomeres from different chromosomes might in part be explained by the assembly of the G-rich strand of telomeres from different chromosomes into G4 DNA, with the bases bonded by Hoogsteen pairing or bonded into G-quartet DNA (Sen and Gilbert, 1988; Williamson *et al.*, 1989; Sundquist and Klug, 1989). Large clusters of telomere repeats may be formed in this manner. Whatever the molecular basis for the assembly of the telomere repeats, we can assume that they generate a structural framework from which chromosomal DNA extends throughout the nuclear interior.

The mini-chromosome specific 177 bp repeats in insect form trypanosomes showed a different distribution from the telomere repeats and were most often confined to less than one half of the nucleus. The 177 bp repeat sequences were found at the nuclear envelope, either in a single band or grouped into several small clusters. The function of the 177 bp repeat is unclear. Since the 177 bp repeat is only located on mini-chromosomes, we consider it unlikely that it is the trypanosomal centromere. We cannot exclude, however, that the mini-chromosomes have a centromere that is different from those of the larger chromosomes.

The interphase nuclei exhibited a few distinct distribution patterns for the same repetitive element. The explanation for this variability may be in an altered spatial organization of chromatin in the transition from telophase to interphase and prophase. This heterogeneity could reflect an organized pattern of chromosomal condensation and decondensation as observed for *Drosophila* embryo nuclei (Hiraoka *et al.*, 1989). The organizational patterns might be explained by the presence of sequence-specific DNA binding proteins which are differentially expressed or undergo secondary modifications during the cell cycle or cell differentiation. The occurrence of discrete nuclear distribution patterns for different repeat families indicates that several different molecular mechanisms must exist to determine the spatial distribution of DNA in the *T.brucei* nucleus. In addition, to confine DNA sequences in separate clusters to specific regions, the nucleus must have polarity.

The organizational patterns are not likely to be an artefact of our fixation and/or hybridization procedures. This conclusion is based on the observations showing that: (i) different fixation techniques, using either a cross-linking agent or a formalin−methanol−acetic acid fixative, gave identical results; (ii) an artefact which specifically generates spatial organization and which clusters homologous sequences in distinct distribution patterns still reflects a higher order structure by which the sequences become compartmentalized; (iii) a comparison of nuclei that were stained with DAPI *in vivo* and nuclei that were stained after hybridization showed similar patterns of staining intensity, indicating that the distribution of the bulk DNA is unaltered following hybridization (data not shown); (iv) the hybridization patterns were reproducible (at least 300 cells were counted for each probe in more than three different experiments).

We have located several other repeated DNA sequences from larger chromosomes [rRNA genes, Van der Ploeg *et al.*, 1990; variant cell surface glycoprotein (VSG) genes, Chung and Van der Ploeg, unpublished] and we have compared their nuclear location to that of the telomeres and mini-chromosomes. These repeated gene families also showed highly organized nuclear locations, most often being grouped into one (rRNA in bloodstream form trypanosomes) or several clusters (VSG genes in bloodstream form trypanosomes) at central nuclear positions. We are currently using dual fluorophere labeling to locate these repetitive gene families relative to the telomere and 177 bp repeats in a single nucleus. From the data presented, we conclude that a high level of spatial organization exists in the interphase *T.brucei* nucleus. The analysis of spatial nuclear organization in higher eukaryotic nuclei will be facilitated by their larger diameter (~10 μm). It can then be established whether a level of organization similar to that found in *T.brucei* applies

to higher eukaryotic nuclei. It is possible that the telomere repeat aggregation is specific for the protozoan *T.brucei* or for nuclei with many chromosomes.

Nuclear compartmentalization may serve a role in the control of gene expression and chromosome and telomere function by affecting the accessibility of DNA and RNA to particular macromolecules. This role has previously been proposed for the nucleolus (for review see Bourgeois and Hubert, 1986), a well defined nuclear structure which functions in rRNA gene expression. Our data indicate that in trypanosome nuclei, many specific sequences are highly compartmentalized, similar to the rRNA genes in the nucleolus. Potential roles that can be ascribed to these structures range from telomere and chromosome functioning and the control of differential gene expression to RNA transport and RNA processing (Lawrence *et al.*, 1988, 1989; Berman *et al.*, 1990; Fu and Maniatis, 1990). Finally, trypanosomes encode a large repertoire of telomerically located VSG genes. The significance of nuclear structure and telomere repeat association in the control of differentially expressed, telomerically located VSG genes is currently being investigated.

Materials and methods

Description of trypanosomes and preparation of cytosmears

The diameter of nuclei from insect form trypanosomes show size reduction when the cultures reach the exponential phase of growth (data not shown). Changes in nuclear volume have previously been reported for *Drosophila* embryo nuclei, following heat shock, O_2 deprivation or changes in the stage of embryo development (Foe and Alberts, 1985). To assure minimal differences in nuclear size, we performed our studies on trypanosomes from mid-log phase cultures.

T.brucei strain 427 stock 60 was used in this study. Variant antigen type 118 clone 1 insect and bloodstream form trypanosomes (Rudenko and Van der Ploeg, 1989; Lee and Van der Ploeg, 1987) have been described previously. Stock 427-60 insect form trypanosomes were originally obtained from Dr R.Brun and have been maintained in SDM79 medium at 24°C as described by Brun and Schonenberger (1979).

Bloodstream form trypanosomes were grown in sublethally irradiated rats and harvested by cardiac puncture at a high level of parasitemia. The blood was mixed with sodium citrate (0.38% final concentration) to prevent clotting. Trypanosomes were separated from red blood cells by centrifugation in a clinical centrifuge at 500 *g* at 37°C for 8 min. The purified trypanosomes were diluted into Baltz medium (Baltz *et al.*, 1985; minimal essential medium supplemented with 10% fetal calf serum, 1% (w/v) glucose and 0.38% sodium citrate) and maintained at 37°C. An aliquot of trypanosomes was washed once in Baltz medium at 37°C, once in Hank's balanced salt solution (HBSS) supplemented with 5% fetal calf serum and 0.38% sodium citrate at 37°C, and diluted in supplemented HBSS to a final concentration of $1-2 \times 10^6$/ml. 100 μl was spun onto clean glass slides primed with supplemented HBSS at 1000 r.p.m. for 10 min at room temperature using a Shandon cytospin.

Insect form trypanosomes were washed twice with HBSS (supplemented with 5% fetal calf serum and 0.38% sodium citrate) at room temperature and spun onto slides as for bloodstream form trypanosomes.

Fixation and storage

Trypanosome cytosmears were fixed by treating them for either: (i) 10 min at −20°C with 2% formalin in 70% methanol and 25% glacial acetic acid, followed by 70% methanol and 25% glacial acetic acid for 5 min and two changes of 75% methanol and 25% glacial acetic acid for 5 min at room temperature; or (ii) 5 min with 2% paraformaldehyde at room temperature, rinsed in 1 × PBS and dehydrated with ethanol. Slides were air dried, wrapped in foil and stored at −70°C with desiccant.

Probes and nick translation

Probes were generated by nick translation of plasmid DNA as previously described, using [biotin-11]dUTP or [biotin-16]dUTP (Van der Ploeg *et al.*, 1984b, 1990). DNA probes were titrated to be smaller than 700 bp following the nick translation.

Hybridization and detection

The procedures for *in situ* hybridization described here are modified from the methods of Lawrence *et al.* (1988, 1989). Prior to hybridization, cytosmears were baked at 60°C for 3 h, incubated for 10 min in 0.1 M triethanolamine and 10 min in acetic anhydride at room temperature and denatured for 2 min at 72°C in 70% deionized, recrystallized formamide (FLUKA), 2 × SSC. The cytosmears were immediately dehydrated for 5 min each in ice-cold 70%, 80%, 90% and 100% ethanol, with stirring, then allowed to air dry. For each sample, 100 ng nick translated plasmid DNA was ethanol co-precipitated, with 5 μg salmon sperm DNA and 20 μg tRNA and was dissolved in 5 μl recrystallized formamide, and spun briefly in a microfuge to remove aggregated material. The probe was heated to 75°C for 10 min, immediately chilled on ice and mixed with an equal volume of cold 2 × hybridization buffer (4 × SSC, 2% BSA and 20% dextran sulfate). After mixing, the probe was applied to the cytosmear and covered to prevent evaporation. Hybridizations were carried out in a moist chamber at 42°C for 16 h. The hybridization mixture was then removed by rinsing the slide in 2 × SSC for 5 min at room temperature. Cytosmears were then washed for 30 min each in 50% deionized recrystallized formamide and 2 × SSC at 37°C, 2 × SSC at 37°C, and 1 × SSC at room temperature. To eliminate hybridization to cytoplasmic and nuclear RNA, cytosmears were treated with 16−20 U/ml of DNase free RNase H (BRL) for 30 min at 37°C in a buffer consisting of 100 mM KCl, 20 mM Tris−HCl (pH 7.5), 1.5 mM $MgCl_2$, 50 μg/ml BSA, 1 mM DTT, 0.7 mM EDTA and 13 mM HEPES (pH 7.5), then washed once in 4 × SSC at room temperature for 10 min.

Streptavidin (Calbiochem) was conjugated to tetramethylrhodamine (TRITC) by the celite method as previously described (Tse *et al.*, 1986). To detect hybridized biotinylated probes, samples were incubated with 50 μg/ml TRITC−streptavidin, 1 mg/ml BSA and 4 × SSC, for 30 min at room temperature in a dark, moist chamber, washed for 10 min in 4 × SSC pH 7.4, then rinsed briefly twice in 1 × SSC pH 7.4.

Nuclear and kinetoplast DNA were detected by staining with 1 μg/ml DAPI for 30 min, rinsed briefly in 1 × SSC pH 7.4 and mounted in Elvanol.

Hybridization conditions and sensitivity

Since post-hybridizational washes were performed at 37°C in 50% formamide and 1 × SSC, only homologous sequences are detected. Hybridization with chromosomal DNA was only observed if the nuclear DNA was denatured prior to the hybridization; each specific probe gave distinguishable and reproducible hybridization patterns; heterologous probes (pBR322, pGEM-3) did not give detectable hybridization signals; hybridization signals derived from RNA were removed by treatment of DNA−RNA hybrids with RNase H (Lawrence *et al.*, 1988; Van der Ploeg *et al.*, 1990).

The sensitivity of detection was determined by comparing the hybridization intensities obtained with a single copy probe (1 kb single copy probe for VSG 118) (no signal), 25 kb single copy probe from the *hsp70* locus (faint signal, distributed into two hybridizing dots per nucleus; probe H1, Glass *et al.*, 1986) and highly repetitive probes for rRNA and VSG genes, telomere repeats and mini-chromosomes (this paper and Van der Ploeg *et al.*, 1990).

Microscopy

Samples were visualized with a 65× water immersion objective, or a 100× oil immersion objective (Leitz P.Fluotar) using a Leitz Diaplan fluorescence microscope with excitation and emission filters specific for visualization of DAPI and rhodamine. Photographs were taken with Kodak Ektachrome 800-1600 color film, processed at 800 or 1600 ASA. Exposure times were generally a few seconds for DAPI fluorescence and up to 40 s for rhodamine.

Confocal microscopy was performed with a Bio-Rad Laser Sharp MRC-500 optical system attached to a Leitz orthoplan microscope. The MRC-500 system is equipped with an argon laser and a motorized focus control for image scanning. The control system of the microscope was coupled to software and hardware configured for an IBM-PC AT compatible computer. The sample manipulation required an image acquisition frame, image processor, software for image smoothing, zooming magnification with contrast enhancement, pseudocolor output, image merging, division and N × N matrix convolution.

The Bio-rad confocal microscope (Wells *et al.*, 1989) has a Z-axis resolution of 1.0 μm FWHM. Closing the aperture allows sampling at shorter intervals. The sampling capability, scanning parameters, and aperture width were determined by scanning fluorescent beads with diameters of 4.5, 0.8, 0.5 and 0.4 μm. We calibrated the depth of field by scanning through the beads and by determining which fluorescent beads were smaller than the depth of field chosen, therefore *not* allowing us to visualize only a section

tion of the bead. Even the 0.4 μm beads were considerably larger than the depth of field chosen at which trypanosomes were scanned.

Since the confocal microscope is not equipped with a laser capable of exciting DAPI (UV range), nuclei were located by inspection of the slides with conventional fluorescence microscopy prior to confocal microscopy.

Every image, independent of the depth of field chosen, was constructed by accumulating 10–15 individual images of the same field which were then superimposed, averaged and enhanced. This procedure increases the accuracy of signal detection and increases the signal to noise ratio.

Acknowledgements

We thank Sylvia Le Blancq, Michael Weiden and Mary Gwo-Shu Lee for critical reading of the manuscript and Piet Borst and Joost Zomerdijk for discussion. This work was supported by a grant to L.H.T.V.D.P. from the National Institutes of Health, no. AI 21784 and a grant from the John D. and Catherine T.MacArthur Foundation and in part by grants to R.N.T., #CA 18506 and CA 42450/01, National Cancer Institute, DHHS and #CH 48585, American Cancer Society, Mathieson Foundation, Melanova Foundation and the Cancer Research League of New York and by a grant from the Department of Medicine special projects Fund from North Shore University Hospital to D.B.T. L.H.T.V.D.P. is a Burroughs Wellcome Scholar in Molecular Parasitology and a recipient of the Hirschl Award and the Searle Scholar Award.

References

Agard,D.A. and Sedat,J.W. (1983) *Nature*, **302**, 676–681.
Baltz,T., Baltz,D., Giroud,C. and Crockett,K. (1985) *EMBO J.*, **4**, 1273–1277.
Berman,S.A., Bursztajn,S., Bowen,B. and Gilbert,W. (1990) *Science*, **247**, 212–214.
Blackburn,E.H. and Challoner,P.B. (1984) *Cell*, **36**, 447–457.
Borden,J. and Manuelidis,L. (1988) *Science*, **242**, 1687–1691.
Borst,P., Fase-Fowler,F.F., Frasch,A.C.C., Hoeijmakers,J.H.J. and Weijers,P.J. (1980) *Mol. Biochem. Parasitol.*, **1**, 221–246.
Borst,P., Van der Ploeg,M., Van Hoek,J.F.M., Tas,J. and James,J. (1982) *Mol. Biochem. Parasitol.*, **6**, 13–23.
Bourgeois,C.A. and Hubert,J. (1986) *Int. Rev. Cytol.*, **3**, 1–52.
Brun,R. and Schonenberger,M. (1979) *Acta Trop.*, **36**, 289–292.
Clayton,C.E. (1988) *Genet. Eng.*, **7**, 2–56.
Comings,D.E. (1980) *Hum. Genet.*, **53**, 131–143.
Cooke,H.J. and Smith,B.A. (1986) *Cold Spring Harbor Symp. Quant. Biol.*, **51**, 213–219.
De Lange,T., Shiue,L., Myers,R.M., Cox,D.R., Naylor,S.L., Killery,A.M. and Varmus,H.E. (1990) *Mol. Cell. Biol.*, **10**, 518–527.
Englund,P.T.S., Hajduk,S.L. and Marini,J.C. (1982) *Annu. Rev. Biochem.*, **51**, 695–726.
Foe,V.E. and Alberts,B. (1985) *J. Cell. Biol.*, **100**, 1623–1636.
Fu,X.-D. and Maniatis,T. (1990) *Nature*, **343**, 437–441.
Gibson,W., Osinga,K.A., Michels,P.A.M. and Borst,P. (1985) *Mol. Biochem. Parasitol.*, **16**, 231–242.
Glass,D.J., Polvere,R.I.P. and Van der Ploeg,L.H.T. (1986) *Mol. Cell. Biol.*, **6**, 4657–4666.
Hancock,R. and Hughes,M.E. (1982) *Biol. Cell.*, **44**, 201–212.
Hiraoka,Y., Minden,J.S., Swedlow,J.R., Sedat,J.W. and Agard,D.A. (1989) *Nature*, **342**, 293–296.
Hochstrasser,M. and Sedat,J.W. (1987) *J. Cell. Biol.*, **104**, 1455–1470.
Lawrence,J.B., Villnave,C.A. and Singer,R.H. (1988) *Cell*, **52**, 51–61.
Lawrence,J.B., Singer,R.H. and Marselle,L.M. (1989) *Cell*, **57**, 493–502.
Lee,M.G.S. and Van der Ploeg,L.H.T. (1987) *Mol. Cell. Biol.*, **7**, 357–364.
Mathog,D., Hochstrasser,M., Gruenbaum,Y., Saumweber,H. and Sedat,J. (1984) *Nature*, **308**, 414–421.
Mathog,D. and Sedat,J.W. (1989) *Genetics*, **121**, 293–311.
Newport,J.W. and Forbes,D.J. (1987) *Annu. Rev. Biochem.*, **56**, 535–565.
Rabl,C. (1885) *Morphologisches Jahrbuch*, **10**, 214–330.
Rudenko,G. and Van der Ploeg,L.H.T. (1989) *EMBO J.*, **8**, 2633–2638.
Sen,D. and Gilbert,W. (1988) *Nature*, **334**, 364–366.
Shotton,D.M. (1989) *J. Cell Sci.*, **94**, 175–206.
Sloof,P., Menke,H., Caspers,M.P.M. and Borst,P. (1983) *Nucleic Acids Res.*, **11**, 3889–3901.
Solari,A.J. (1980) *Chromosoma (Berl.)*, **78**, 239–255.
Solari,A.J. (1982) *J. Protozool.*, **29**, 330–331.
Solari,A.J. (1983) *Z. Parasitenkund.*, **69**, 3–16.
Sundquist,W.I. and Klug,A. (1989) *Nature*, **342**, 825–829.
Szostak,J.W. and Blackburn,E.H. (1982) *Cell*, **29**, 245–255.
Tse,B.D., Al-Haideri,M., Pernis,B., Cantor,C.R. and Wang,C.Y. (1986) *Science*, **234**, 748–751.
Van der Ploeg,L.H.T., Schwartz,D., Cantor,C.R. and Borst,P. (1984a) *Cell*, **39**, 213–221.
Van der Ploeg,L.H.T., Cornelissen,A.W.C.A., Michels,P.A.M. and Borst,P. (1984b) **Cell**, **37**, 77–84.
Van der Ploeg,L.H.T., Liu,A.Y.C. and Borst,P. (1984c) *Cell*, **36**, 459–468.
Van der Ploeg,L.H.T., Smith,C.L.S., Polvere,R.I. and Gottesdiener,K. (1989) *Nucleic Acids Res.*, **17**, 3217–3227.
Van der Ploeg,L.H.T., Tse,D.B., Shea,C., Lee,G.-S.M., Huang,J., Weiden,M., Rudenko,G., Gottesdiener,K., Klco,S., Brown,S., Chung,H.-M.M., Bishop,D. and Rattray,A. (1990) In Van der Ploeg,L.H.T., Cantor,C.R. and Vogel,H.J. (eds), *Immune Recognition and Evasion: Molecular Aspects of Host-parasite Interaction.* Academic Press, San Diego, in press.
Van der Ploeg,L.H.T. (1990) In Hames,B.D. and Glover,D.M. (eds), *Frontiers in Molecular Biology. Genomic Rearrangements and Amplification.* IRL Press, Oxford, 51–97.
Wells,K.S., Sandison,D.R., Strickler,J. and Webb,W.W. (1989) In Pawley,J. (ed.), *Confocal Microscopy Handbook.* EMSA, San Antonio, pp. 23–35.
Williamson,J.R., Raghuraman,M.K. and Cech,T. (1989) *Cell*, **59**, 871–880.

Received on March 1, 1990; revised on April 24, 1990